ADVANCED FUNCTIONAL MATERIALS
www.afm-journal.de

Accelerated Iron Oxide Nanoparticle Degradation Mediated by Polyester Encapsulation within Cellular Spheroids

*Brandon Mattix, Timothy R. Olsen, Thomas Moore, Megan Casco, Dan Simionescu, Richard P. Visconti, and Frank Alexis**

Nanomaterials including gold nanoparticles, polymeric nanoparticles, and magnetic iron oxide nanoparticles are utilized in tissue engineering for imaging, drug delivery, and maturation. Prolonged presence of these nanomaterials within biological systems remains a concern due to potential adverse affects on cell viability and phenotype. Accelerating nanomaterial degradation within biological systems is expected to reduce the potential adverse effects in the tissue. Similar to biodegradable polymeric scaffolds, the ideal nanomaterial remains stable for sufficient time to accomplish its desired task, and then rapidly degrades once that task is completed. Here, surface modifications are reported to accelerate iron oxide MNP degradation mediated by polymer encapsulation, in which iodegradable coatings composed of FDA approved polymers with different degradation rates are used: poly(lactide) (PLA) or copolymer poly(lactide-co-glycolide) (PLGA). Results demonstrate that degradation of MNPs can be controlled by varying the content and composition of the polymeric nanoparticles used for MNP encapsulation (PolyMNPs). Incorporated into cellular spheroids, PolyMNPs maintain a high viability compared to non-coated MNPs, and are also useful in magnetically patterning cellular spheroids into fused tissues for tissue engineering applications. Accelerated degradation compared to non-coated MNPs makes PolyMNPs a viable alternative for removing nanomaterials from tissues after accomplishing their desired role.

1. Introduction

A variety of nanomaterials, including gold nanoparticles, carbon nanotubes, polymeric nanoparticles, and magnetic iron oxide nanoparticles, have been used in various tissue engineering strategies involving imaging, tissue maturation and integration, and drug delivery.[1–9] Magnetic nanoparticles (MNPs) are now being increasingly used in biomedical applications,[10–20] with some U.S. Food and Drug Administration approved iron oxide MNP formulations used to treat iron deficiency (Feraheme) or as MRI contrast agents (Feridex).[21–23] MNPs have been investigated in tissue engineering applications for in vivo cell tracking,[24–29] in vivo monitoring of transplanted tissues,[30–32] cell and tissue patterning,[11,13,15] and tissue maturation.[33] However, the prolonged presence of MNPs can induce adverse effects in cells, causing cell toxicity, and changes in both cell phenotype and cell mobility.[13,34,35] Though the surface functionalization or coating of MNPs in oleates,[36,37] dextran,[23,38] or polymers[31,39] can improve MNP biocompatibility, they do not control the MNP degradation. Ideally, MNPs will remain stable for a sufficient time to accomplish their desired task, and then rapidly degrade once their task is completed.

A variety of different chemicals, primarily organic acids, have been investigated to accelerate the degradation of iron oxide MNPs.[40–44] In these experiments, after the MNPs accomplished their desired task, the accelerated MNP degradation decreased their interaction with cells. Here, we report the precise control of iron oxide MNP degradation via MNP encapsulation within biodegradable polymers for tissue engineering applications. Iron oxide MNPs encapsulated within polymeric nanoparticles are a biodegradable alternative to non-coated MNPs to remove MNP in situ in that they obviate potential toxicities. By accelerating MNP degradation, they may have broad use in medical devices, drug delivery, and bioimaging agents composed of iron oxides.

B. Mattix, T. R. Olsen, T. Moore,
M. Casco, Dr. D. Simionescu, Dr. F. Alexis
Department of Bioengineering
Clemson University 301 Rhodes Research Center
Clemson, SC, 29634, USA
E-mail: falexis@clemson.edu
Dr. R. P. Visconti
Department of Regenerative Medicine and Cell Biology
Medical University of South Carolina
Charleston, SC, 29425, USA

DOI: 10.1002/adfm.201301736

2. Results and Discussion

MNPs were loaded into polymeric nanoparticles using a solvent evaporation technique with two different polymers, poly(lactide)-poly(ethylene glycol) (PLA-PEG) and poly(lactide-co-glycolide)-poly(ethylene glycol) (PLGA-PEG), and purified to eliminate free polymer and MNPs to form PolyMNPs (**Figure 1**A). The generation of polymer degradation byproducts, lactic and glycolic acid, created an acidic microenvironment

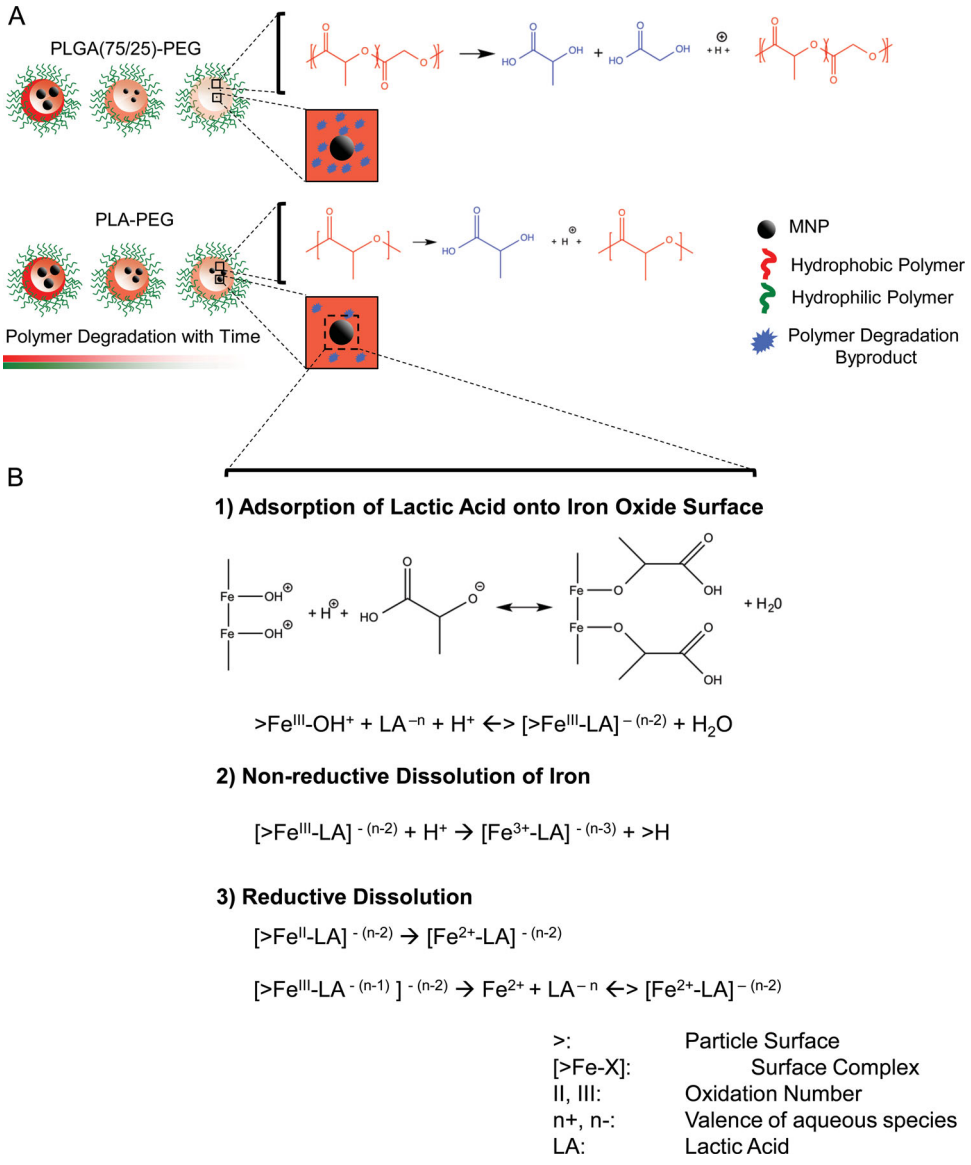

Figure 1. Iron oxide degradation. A) MNPs were encapsulated within polymeric nanoparticles prepared using the conventional nanoprecipitation method. Two different polymers, PLA-PEG and PLGA(75/25)-PEG, were used to prepare PolyMNPs. As both degrade at different rates, they generate a differential content of polymer degradation byproducts such as lactic acid and glycolic acid. B) Schematic of the dissolution of iron oxide by acids, specifically polymer degradation byproducts lactic acid and glycolic acid, which occurs in three primary steps: adsorption of organic ligands on the iron oxide surface, non-reductive dissolution, and finally reductive dissolution.[44]

within the polymeric nanoparticles (NPs).[45] Furthermore, the dissolution of iron oxide by acids occurred in three primary steps: the adsorption of organic ligands on the iron oxide surface, then non-reductive dissolution, and finally reductive dissolution (Figure 1B).[44] FT-IR analysis showed that MNPs were encapsulated into polymeric NPs with a carbonyl stretch peak at 1745 cm^{-1} corresponding to the ester bond in PLA (**Figure 2**A). Thermogravimetric analysis (TGA) was used to quantify the relative weight percent of polymer composition of PolyMNPs formulations. By varying the MNP:polymer weight ratios at 1:1.85, 1:5, and 1:10, we achieved 20, 25, and 33 wt% polymer, respectively (Figure 2B). Furthermore, transmission electron microscopy (TEM) analysis showed that the encapsulation of MNPs within polymeric NPs (300 nm) lead to a slight increase in NP diameter compared to unloaded polymeric NPs (100–150 nm, Figure 2C). The TEM images suggest that MNPs are associated with polymeric NPs and could possibly populate the outer parts of the NPs. The degradation kinetics for the two polymers used for encapsulation, PLA-PEG and PLGA(75/25)-PEG, were obtained via gel permeation chromatography (GPC). Results indicated a variance in polymer degradation based upon polymer composition (Supporting Information, Figure S1). PLGA(75/25)-PEG molecular weight (M_w) decreased faster compared to PLA-PEG, losing roughly 20% of its initial M_w after 2

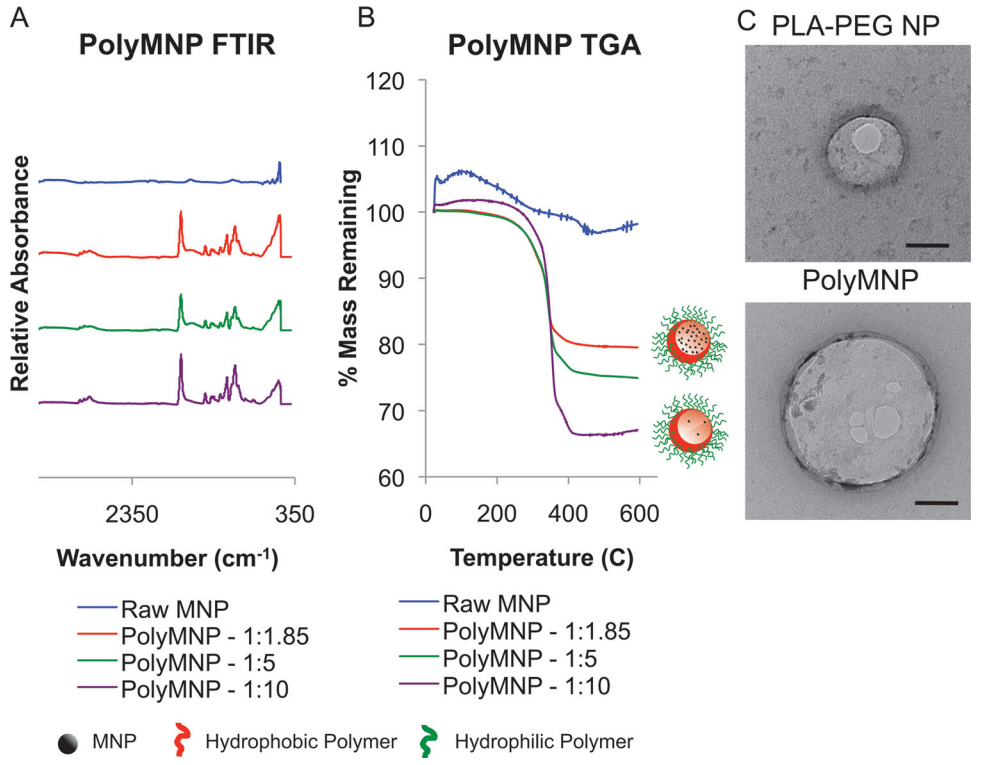

Figure 2. PolyMNP characterization. A) Using PLA-PEG nanoparticles, polymer encapsulation of PolyMNPs was tested for three MNP:polymer ratios: 1:1.85, 1:5, and 1:10. FT-IR showed the presence of PLA-PEG for all three formulations of the PolyMNP assembly compared to the non-encapsulated MNP control. B) Thermogravimetric analysis was performed to determine the polymer:MNP content. Results showed that the lowest MNP:polymer ratio (1:1.85) correlated to the highest MNP content, while the highest MNP:polymer ratio (1:10) corresponded to the lowest MNP content. C) TEM analysis confirmed the nanostructure of NPs. Results showed an increase in diameter for 1:10 PLA-PEG PolyMNPs (300 nm) compared to unloaded polymeric NPs (100–150 nm). Scale bar = 100 nm.

weeks in PBS at 37 °C due to its copolymer composition and higher hydrophilicity.[46,47] PLA-PEG lost approximately 10% of its initial M_w under the same conditions. By tailoring the degradation kinetics of polymeric NPs, it is possible to control the MNP degradation rate due to the increased content of oligomer residues from polymer degradation at the interface of iron oxide MNPs and the polymer coating. Polymeric microparticles and nanoparticles were observed to degrade over time, forming a local acidic microenvironment generated from degradation byproducts including lactic and glycolic acid. The formation of a local acidic core within polymeric NPs has been shown.[45,48] Furthermore, Miller et al. confirmed that lactic acid (0.1 M), a degradation byproduct of PLA, led to dissociation of iron oxide after 100 h at room temperature, demonstrating roughly 80% degradation at pH 3.5 but only 10% degradation at pH 5.5.[43] However, other studies have shown that the use of lactic acid (0.12–0.16 M) to expose cells to pH 5.7 or below induced cell toxicity.[49] Therefore, the use of polymeric NPs to encapsulate MNPs permits the control of a local acidic microenvironment within the degrading polymer NP that will in turn accelerate encapsulated MNP degradation.

The encapsulation of MNPs within polymeric NPs accelerated MNP degradation, and MNP degradation was controlled by varying the polymer composition. Using 1:5 PolyMNP conditions, the degradation of MNPs encapsulated into both PLGA(75/25)-PEG and PLA-PEG NPs was measured after incubating PolyMNPs within cellular spheroids.[50] Briefly, PolyMNP cellular spheroids were first treated with 5 M HCl to dissociate MNPs within cellular spheroids, followed by quantification of the free iron within the HCl solutions using a Perl's Prussian blue colorimetric technique. PolyMNP degradation was compared to non-encapsulated MNP degradation over the course of 21 days. PLGA(75/25)-PEG PolyMNPs caused a 15% degradation of the initial iron content, while PLA-PEG PolyMNPs showed only a 7% degradation and non-coated MNPs only a 4% degradation over the same time period (**Figure 3**A). These results, which correlate with the polymer degradation rates (Supporting Information, Figure S1), showed that the PLGA(75/25)-PEG degraded more quickly than PLA-PEG. Polymer degradation is in part controlled by the differential hydrophilicity in the polymer composition. Increasing the polymer degradation rate is expected to more rapidly increase the content of the acidic monomer and oligomer byproducts at the MNP interface.[45,46,51] Conversely, a slower degradation of polymers is expected to slowly degrade MNPs due to a lower content of acidic monomer and oligomer byproducts. The degradation of PolyMNPs was further qualitatively confirmed by histological staining of cellular spheroids over the course of 40 days using H&E and Lillie's Turnbull Reaction to highlight iron oxide MNPs (Figure 3B, PLA-PEG PolyMNPS, Supporting

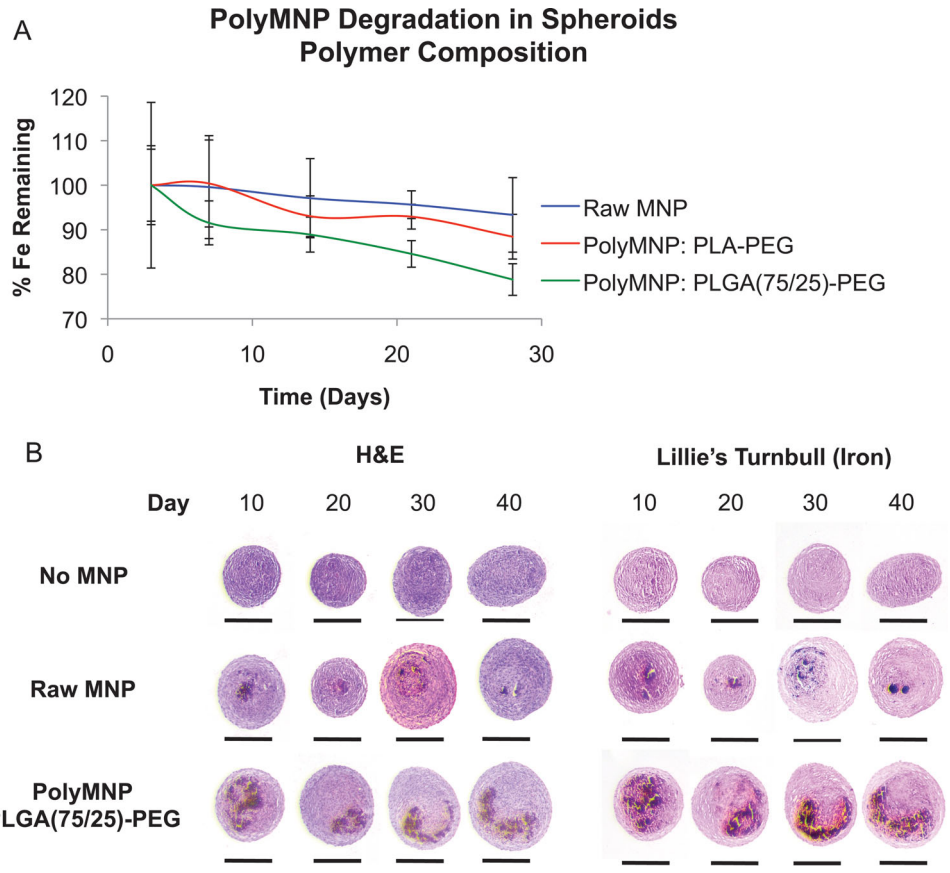

Figure 3. Effect of polymer composition on PolyMNP degradation. A) Two polymers possessing different degradation rates were used to prepare PolyMNPs: PLA-PEG and PLGA(75/25)-PEG. A Perl's reagent (potassium ferrocyanide) assay was used to measure the degradation of PolyMNPs encapsulated into both polymer nanoparticles after incubation of PolyMNPs within cellular spheroids.[50] An analysis of that degradation within cellular spheroids showed that polymer degradation rates mediate MNP degradation. PLGA(75/25)-PEG PolyMNPs, the fastest degrading polymer of the two formulations tested, demonstrated the most accelerated MNP degradation compared to PLA-PEG PolyMNPs and non-encapsulated MNP controls over the course of 21 days. B) Degradation of PolyMNPs was also qualitatively analyzed using histological staining (H&E and Lillie's Turnbull for iron) over the course of 40 days. Results showed that PolyMNPs dissociate into smaller aggregates over time, correlating with MNP degradation quantitative analysis (Scale bar = 500 μm).

Information, Figure S2). Results showed that similar to non-encapsulated MNPs, PolyMNPs dissociate over time into smaller aggregates of MNPs, a dissociation that corresponds to a degradation of the MNPs shown in Figure 3A.[41] A primary concern of using MNPs for tissue engineering is their long-term presence in human tissues, which often induce adverse effects on surrounding cells. A safe method that can accelerate this MNP degradation, however, is expected to limit the interaction of MNPs with the biological environment, which is critical in reducing cytotoxicity. The presented results confirm that the polymer composition of PolyMNPs can control the degradation rate of MNPs in physiological conditions. This accelerated degradation, compared to non-encapsulated MNPs, makes PolyMNPs most appealing for use as MNPs in biomedical applications that necessitate limited interaction with the biological environment.

The effect of polymer content to PolyMNP degradation was subsequently analyzed. By varying the relative content of polymer encapsulating MNPs within polymeric NPs, we controlled the rate of MNP degradation. By increasing the content of polymer, we created less MNPs within the polymeric NPs and accelerated MNP degradation (**Figure 4**). As mentioned earlier, TGA results showed that by varying MNP:polymer weight ratios during synthesis (Figure 2B), we controlled the content of polymer encapsulation of MNPs. Having a higher content of polymer encapsulating MNPs within NPs is expected to increase MNP degradation because of the higher content of monomer and oligomer degradation byproducts.[52] Therefore, the results suggest that the increased presence of degradation byproducts accelerates MNP degradation.[45] Specifically, in experiments using cellular spheroids with PolyMNPs prepared with 1:10 (lowest loading, 33 wt% polymer) and 1:1.85 (highest loading, 20 wt% polymer), we observed a 36% and 7% reduction of their initial iron content after 21 days, respectively. These results indicate that MNP degradation can be tailored by both polymer composition and content.

Since magnetic cellular spheroids are used as components in tissue engineering applications to assemble complex tissues

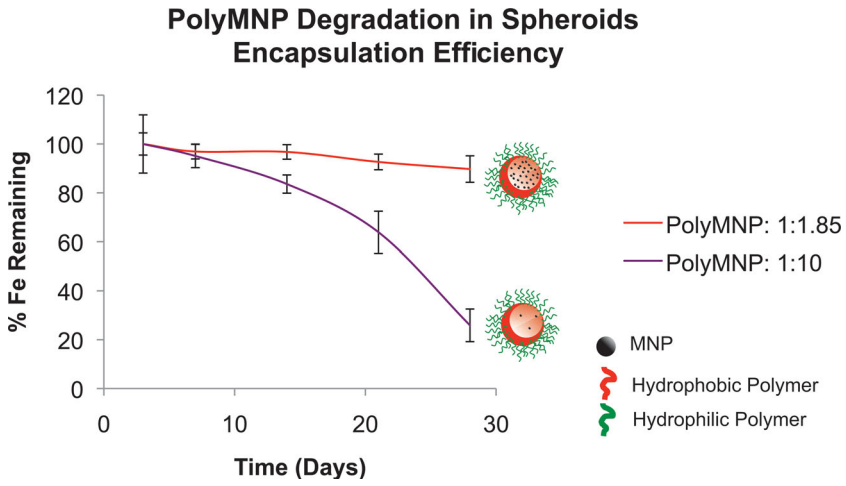

Figure 4. Effect of polymer content on PolyMNP degradation. Using PLA-PEG PolyMNPs, a degradation analysis was performed to determine the effect of polymer content on MNP degradation. The degradation of PolyMNPs composed of 1:1.85, 1:5, and 1:10 MNP:polymer ratios was analyzed over the course of 21 days in cellular spheroids using a Perl's reagent assay.[50] Results showed that PolyMNPs with the highest polymer content correlated to the most accelerated degradation over the course of 21 days, because of the increase in monomer and oligomer degradation byproducts within polymeric nanoparticles.

via magnetic force assembly,[53–55] which causes prolonged MNP and cell interactions, we analyzed PolyMNP cytotoxicity. PolyMNPs assembled using PLA-PEG and PLGA(75/25)-PEG polymeric NPs, and were incorporated into magnetic cellular spheroids and analyzed for cytotoxicity over a period of two weeks. PolyMNPs, 0.5 mg mL^{-1}, maintained high viability until the end of that time for both PolyMNP formulations, compared to control spheroids without MNPs (**Figure 5**A). Furthermore, compared to spheroids composed of cells which internalized raw MNPs, PLGA(75/25)-PEG PolyMNP spheroids maintained a high viability compared to control spheroids without MNPs up to one week (Supporting Information, Figure S3). Raw MNP spheroids showed viability below 20%, compared to control spheroids. Additionally, magnetic cellular spheroids with PolyMNPs were used to magnetically pattern and assemble fused tissues (Figure 5B). Tissue rings, 2 mm in diameter, were successfully patterned and assembled using both PolyMNP formulations, with an equivalent fusion compared to non-encapsulated MNPs. Magnetic cellular spheroids containing PolyMNPs were magnetically patterned and fused together over the course of 48 h, with fused tissue observed after the removal of the magnetic template. These results demonstrated that PolyMNPs maintain high cellular viability and promoted fusion, suggesting that PolyMNPs are a biodegradable alternative to non-encapsulated MNPs for tissue engineering applications.

3. Conclusions

Results showed that the degradation of MNPs can be controlled by the polymeric microenvironment. It was further demonstrated that the degradation rate of MNPs within cellular spheroids can be controlled by varying the polymer composition and content of PolyMNPs. Additionally, high cell viability

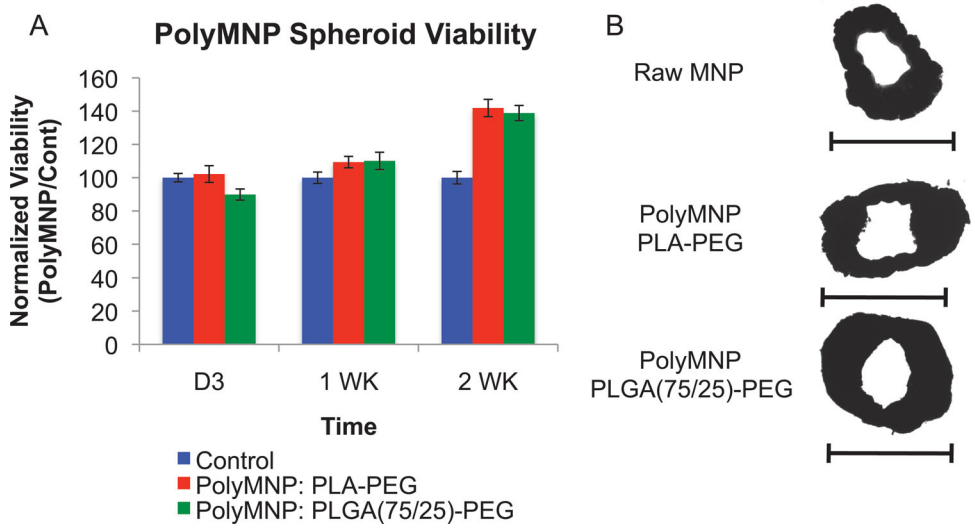

Figure 5. PolyMNPs integrated within cellular spheroids. A) The effect of PolyMNPs on cellular spheroid viability was analyzed to determine the suitability of PolyMNPs for prolonged cellular interaction. Results showed that PolyMNPs (0.5 mg mL^{-1}) can be incorporated into cellular spheroids and maintain high viability compared to MNP-free controls for up to two weeks. B) Furthermore, PolyMNP-containing cellular spheroids were magnetically patterned and assembled into fused tissue rings. Twenty-five individual PolyMNP spheroids were patterned and fused over the course of 48 hours, at which point the magnet pattern was removed and the samples imaged. Results showed a fused tissue construct, confirming that PolyMNPs can be used to assemble fused tissue rings with equivalent fusion compared to non-encapsulated MNP controls.

was maintained in magnetic cellular spheroids up to two weeks, which is a most desirable characteristic of these spheroids for use as constituents for tissue engineering applications requiring prolonged interaction between MNPs and cells. Finally, PolyMNP spheroids were magnetically patterned to promote fusion into homogenous tissues, confirming that magnetic force assembly can be used to pattern PolyMNPs. These results demonstrated that the polymeric microenvironment could be used to precisely control the degradation of MNPs in physiological conditions, which will limit the interaction of MNPs with cells. Consequently, this process is invaluable in creating methods to use MNPs in medical applications, in drug delivery, and as bioimaging agents composed of iron oxide. Future research will entail the use of different polymers for PolyMNP encapsulation, an analysis of the molecular changes at the interface between MNPs and polymers, and a study of the degradation of macrostructures.

4. Experimental Section

Materials: Commercial MNPs (Fe_3O_4, 20–30 nm) were supplied by SkySpring Nanomaterials, Inc. D,l lactide ($C_6H_8O_4$, PURASORB DL) was supplied by Purac Biomaterials. Glycolide ($C_4H_4O_4$, >99%), tin(II) 2-ethylhexanoate ($[CH_3(CH_2)_3CH(C_2H_5)CO_2]_2Sn$, ≈95%), sodium sulfate (Na_2SO_4,, >99%), anhydrous magnesium sulfate ($MgSO_4$, >99.5%), anhydrous toluene ($C_6H_5CH_3$, 99.8%), methanol (CH_3OH, >99.9%), chloroform ($CHCl_3$, >99.8%), and potassium ferrocyanide ($K_4Fe(CN)_6$ □$3H_2O$, 98.5–102.5%) were supplied by Sigma-Aldrich. Methoxy-poly(ethylene glycol) was supplied by JenKem Technology USA (M-PEG-OH, M_w 5000). Acetonitrile (C_2H_3N, 99.9%) and Tetrahydrofuran (C_4H_8O,, 99.9%) were supplied by Fisher Scientific. Hydrochloric acid (HCl, 6 N) was supplied by Ricca Chemical Company. PrestoBlue Cell Viability Reagent and Collagen, Type I Bovine were supplied by Life Technologies.

Polymer Synthesis and Characterization: Reagents used for the polymer synthesis were vacuum-dried (28 in Hg) overnight before use. Block copolymers of PLA-PEG or PLGA-PEG were synthesized via ring opening polymerization using methoxy-poly(ethylene glycol) as the initiator and tin(II) 2-ethylhexanoate as the catalyst.[56] Briefly, mPEG, monomer (i.e., d,l lactide or glycolide), and Na_2SO_4 were vacuum-dried overnight before use. PLGA composition was controlled by varying the ratio of d,l lactide and glycolide. Reagents were dissolved by stirring in 120 °C anhydrous toluene under N_2 gas and reflux. Tin(II) 2-ethylhexanoate was added and reaction vessel was stirred at 120 °C for 24 h under N_2 and reflux. The next day, polymer product was washed in chloroform/water, dried over $MgSO_4$, and precipitated in cold methanol. NMR was performed with a Bruker Avance 300. ^{1}H NMR (300 MHz, $CDCl_3$, δ): 7.26 (s, $CDCl_3$), 5.17 (q, –C(=O)–CH(CH_3)–), 4.82 (d, –C(=O)–CH_2–O–), 3.65 (s, –CH_2CH_2–O–), 1.59 (d, –CH(CH_3)–). ATR FT-IR was performed with a Thermo-Nicolet Magna 550 equipped with a Thermo-SpectraTech Foundation series Endurance Diamond ATR. IR: 2881 cm^{-1} (–CH_2CH_2–O–), 1745 cm^{-1} (C=O). TGA was performed on a TA Instruments Hi-Res TGA 2950 thermogravimetric analyzer under nitrogen from 25 °C to 600 °C at 20 °C min^{-1}. TEM images were obtained using a Hitachi 7600 microscope at 120 kV. NPs and PolyMNPs (1 mg mL^{-1}) were suspended in water and dropped onto carbon-formvar copper grids (Electron Microscopy Sciences) and counter-stained using 5% uranyl acetate (90 min, wash in water) prior to imaging.[57]

Polymer Degradation: Polymers were dissolved in acetonitrile (ACN, 50 mg mL^{-1}) and dispensed into a non-treated 96-well plate (125 µL, 6.25 mg). Plates were left overnight under a chemical hood to evaporate ACN, leaving behind a polymer film. Wells were filled with PBS and incubated at 37 °C until their respective time point. At each time point, PBS was removed and samples were washed three times with Hyclone Molecular Biology Grade Water (Fisher Scientific). Samples were dissolved in ACN and collected to be dried via lyophilization. The Polymer Molecular Weight was determined through gel permeation chromatography (GPC) on a Waters 1525 Binary HPLC pump with a Waters 2414 refractive index detector. A Shodex KF-804L column (8.0 mm × 300 mm, ID × Length) and Shodex KF guard column were used for separation. The mobile phase was tetrahydrofuran (THF) and polymers were prepared by dissolving in THF at a concentration of 1 mg mL^{-1} and filtering through a 0.2 µm PTFE syringe filter (VWR International). Flow rate was set at 1 mL min^{-1} and polystyrene standards (Poly-Sciences) were used to quantify molecular weight using a third-order fit calibration curve. The MW of samples at each time point was expressed as a percent initial.

PolyMNP Encapsulation: MNPs were encapsulated into polymeric nanoparticles via solvent evaporation.[58] Briefly, equal volumes of polymer (5 mg mL^{-1}) and iron oxide were dispersed in ACN and combined with Hyclone Molecular Biology Grade Water at a 1:2 ratio. Solutions were stirred for two hours.

Cell Culture: Primary rat aortic smooth muscle cells (SMCs) were used for all cellular spheroid studies. Cells were cultured in monolayer cultures using Dulbeco's Modified Eagle Medium:F-12 (ATCC, 1:1, DMEM:F-12) supplemented with 10% fetal bovine serum (Atlanta Biologics) and 1% penicillin-streptomycin-amphotericin (MediaTech, Inc.) at 37 °C and 5% of CO_2.

PolyMNPs in Cellular Spheroids: Equal volumes of solutions containing PolyMNPs, collagen, and SMCs in media were combined and dispensed using a modified hanging drop method. Collagen was pH balanced according to manufacturer recommendations and kept on ice prior to use. Cellular spheroids were assembled using 20 000 cells, 17 µg mL^{-1} collagen, and various PolyMNP concentrations, dependent on the application.

Quantification of PolyMNP Degradation: Iron content within cellular spheroids was quantified using an established technique to quantify that content in solutions.[50] Briefly, MNPs were first dissociated using 5 M HCl, followed by quantification of free iron within solutions using a Perl's Prussian blue colorimetric technique. Magnetic cellular spheroids containing PolyMNPs (0.13–0.2 mg mL^1) were fabricated and incubated in non-treated 96-well plates in cell culture media with media changes every other day. At each time point, cellular spheroids were transferred to 1 mL of sterile PBS in a sterile 1.5 mL microcentrifuge tube to wash samples. Spheroids were then transferred into 100 µL fresh PBS in a non-treated 96-well plate. 100 µL of 5 M HCl was added to each well and incubated at 37 °C for 72 h to dissociate MNPs. Next, 100 µL of 5% potassium ferrocyanide was added to each well and incubated for 15 min at room temperature, with absorbance measurements recorded at 630 nm for each well.

Cellular Spheroid Viability: PolyMNP cellular spheroids were fabricated with 0.5 mg mL^{-1} PolyMNP and compared to control cellular spheroids without PolyMNPs. PrestoBlue cell viability assays were performed to quantify cell viability (at least 3 repeats per sample). Spheroids were first dissociated via incubation with collagenase (100 U mL^{-1}) for 80 min at 37 °C (Collagenase Type IV, Life Technologies), followed by incubation with trypsin (0.25%, Thermo Scientific) for 10 min at 37 °C. Cellular spheroids were then physically dissociated and allowed to adhere overnight on a tissue culture treated 12-well plate.

Histology: PolyMNP cellular spheroids were processed and sectioned via standard paraffin sectioning techniques. Samples were dehydrated using ethanol and xylene prior to being embedded in paraffin. Sections 5 µm thick were stained with hematoxylin and eosin, and Lillie's Technique for Turnnbulls Blue Reaction (Poly Scientific).

Magnetic Patterning and Fusion: Axially magnetized ring magnets (SuperMagnetMan, 2 mm OD, 1 mm ID) were commercially purchased and secured to the bottom of glass chamber slides containing coverglass bottoms. Twenty-five magnetic cellular spheroids (0.14 mg mL^{-1} PolyMNP) were placed in the chamber and allowed to magnetically align. Samples were incubated at 37 °C with 5% CO_2 for 48 h. Magnets were removed after 48 h and samples imaged using a Nikon AZ100 multizoom microscope.

Supporting Information

Supporting Information is available from the Wiley Online Library or from the author.

Acknowledgements

B.M. and T.R.O. contributed equally to this work. This work was supported by American Heart Association Beginning Grant in Aid-2BGIA11720004 award, SC EPSCoR Grant for Exploratory Academic Research, and NSF/EPSCOR EPS-0447660. The authors wish to acknowledge the assistance of Dr. Terri Bruce, Rhonda Powell, and the Clemson Light Imaging Facility at Clemson University for technical support with the microscopy, Linda Jenkins for her assistance with histological techniques, Kim Ivey for help with TGA and FT-IR, and the Clemson Electron Microscope Facility.

Received: May 21, 2013
Revised: August 2, 2013
Published online: September 18, 2013

[1] S. P. Grogan, C. Pauli, P. Chen, J. Du, C. B. Chung, S. D. Kong, C. W. Colwell Jr., M. K. Lotz, S. Jin, D. D. D'Lima, *Tissue Eng. Part C, Methods* **2012**, *18*, 496.
[2] U. A. Gurkan, S. Tasoglu, D. Kavaz, M. C. Demirel, U. Demirci, *Adv. Healthcare Mater.* **2012**, *1*, 149.
[3] S. H. Ku, M. Lee, C. B. Park, *Adv. Healthcare Mater.* **2013**, *2*, 244.
[4] H. Ma, J. Hu, P. X. Ma, *Adv. Funct. Mater.* **2010**, *20*, 2833.
[5] J. Shi, A. R. Votruba, O. C. Farokhzad, R. Langer, *Nano Lett.* **2010**, *10*, 3223.
[6] S. R. Shin, S. M. Jung, M. Zalabany, K. Kim, P. Zorlutuna, S. B. Kim, M. Nikkhah, M. Khabiry, M. Azize, J. Kong, K. T. Wan, T. Palacios, M. R. Dokmeci, H. Bae, X. S. Tang, A. Khademhosseini, *ACS Nano* **2013**.
[7] A. Skardal, J. Zhang, L. McCoard, S. Oottamasathien, G. D. Prestwich, *Adv. Mater.* **2010**, *22*, 4736.
[8] G. Wei, P. X. Ma, *Adv. Funct. Mater.* **2008**, *18*, 3568.
[9] X. Yang, J. J. Grailer, S. Pilla, D. A. Steeber, S. Gong, X. Shuai, *Biofabrication* **2010**, *2*, 025004.
[10] A. Bakandritsos, G. Mattheolabakis, G. Chatzikyriakos, T. Szabo, V. Tzitzios, D. Kouzoudis, S. Couris, K. Avgoustakis, *Adv. Funct. Mater.* **2011**, *21*, 1465.
[11] A. Bratt-Leal, K. L. Kepple, R. L. Carpenedo, M. T. Cooke, T. C. McDevitt, *Integrative Biol.* **2011**.
[12] V. H. B. Ho, W. M. Guo, C. L. Huang, S. F. Ho, S. Y. Chaw, E. Y. Tan, K. W. Ng, J. S. C. Loo, *Adv. Healthcare Mater.* **2013**, unpublished.
[13] V. H. B. Ho, K. H. Müller, A. Barcza, R. Chen, N. K. H. Slater, *Biomaterials* **2010**, *31*, 3095.
[14] U. Jeong, X. Teng, Y. Wang, H. Yang, Y. Xia, *Adv. Mater.* **2007**, *19*, 33.
[15] R.-Z. Lin, W.-C. Chu, C.-C. Chiang, C.-H. Lai, H.-Y. Chang, *Tissue Eng. Part C: Methods* **2008**, *14*, 197.
[16] R. A. Rezende, F. S. Azevedo, F. D. Pereira, V. Kasyanov, X. Wen, J. V. L. de Silva, V. Mironov, *J. Nanotechnol.* **2012**, 2012.
[17] T. Sasaki, N. Iwasaki, K. Kohno, M. Kishimoto, T. Majima, S. I. Nishimura, A. Minami, *J. Biomed. Mater. Res. Part A* **2007**, *86*, 969.
[18] K. Shimizu, A. Ito, M. Arinobe, Y. Murase, Y. Iwata, Y. Narita, H. Kagami, M. Ueda, H. Honda, *J. Biosci. Bioeng.* **2007**, *103*, 472.
[19] K. Shimizu, A. Ito, H. Honda, *J. Biosci. Bioeng.* **2007**, *104*, 171.
[20] G. R. Souza, J. R. Molina, R. M. Raphael, M. G. Ozawa, D. J. Stark, C. S. Levin, L. F. Bronk, J. S. Ananta, J. Mandelin, M. M. Georgescu, J. A. Bankson, J. G. Gelovani, T. C. Killian, W. Arap, R. Pasqualini, *Nat. Nanotechnol.* **2010**, *5*, 291.
[21] A. Figuerola, R. Di Corato, L. Manna, T. Pellegrino, *Towards Clinical Applications of Nanoscale Medicines* **2010**, *62*, 126.
[22] R. A. Heesakkers, G. J. Jager, A. M. Hovels, B. de Hoop, H. C. van den Bosch, F. Raat, J. A. Witjes, P. F. Mulders, C. H. van der Kaa, J. O. Barentsz, *Radiology* **2009**, *251*, 408.
[23] C. Tassa, S. Y. Shaw, R. Weissleder, *Acc. Chem. Res.* **2011**, *44*, 842.
[24] S. A. Anderson, J. Glod, A. S. Arbab, M. Noel, P. Ashari, H. A. Fine, J. A. Frank, *Blood* **2005**, *105*, 420.
[25] J. Basu, C. W. Genheimer, K. I. Guthrie, N. Sangha, S. F. Quinlan, A. T. Bruce, B. Reavis, C. Halberstadt, R. M. Ilagan, J. W. Ludlow, *Tissue Eng. Part C, Methods* **2011**, *17*, 843.
[26] D. Fayol, N. Luciani, L. Lartigue, F. Gazeau, C. Wilhelm, *Adv. Healthcare Mater.* **2013**, *2*, 313.
[27] C.-W. Lu, Y. Hung, J.-K. Hsiao, M. Yao, T.-H. Chung, Y.-S. Lin, S.-H. Wu, S.-C. Hsu, H.-M. Liu, C.-Y. Mou, C.-S. Yang, D.-M. Huang, Y.-C. Chen, *Nano Lett.* **2007**, *7*, 149.
[28] S. H. Wang, X. Shi, M. Van Antwerp, Z. Cao, S. D. Swanson, X. Bi, J. R. Baker, *Adv. Funct. Mater.* **2007**, *17*, 3043.
[29] H. H. P. Yiu, H.-j. Niu, E. Biermans, G. van Tendeloo, M. J. Rosseinsky, *Adv. Funct. Mater.* **2010**, *20*, 1599.
[30] N. V. Evgenov, Z. Medarova, G. Dai, S. Bonner-Weir, A. Moore, *Nat. Med.* **2006**, *12*, 144.
[31] H. Huang, Q. Xie, M. Kang, B. Zhang, H. Zhang, J. Chen, C. Zhai, D. Yang, B. Jiang, Y. Wu, *Nanotechnology* **2009**, *20*, 365101.
[32] H. Skaat, O. Ziv-Polat, A. Shahar, D. Last, Y. Mardor, S. Margel, *Adv. Healthcare Mater.* **2012**, *1*, 168.
[33] J. Dobson, S. H. Cartmell, A. Keramane, A. J. E. Haj, *IEEE Transactions on NanoBioscience* **2006**, *5*, 173.
[34] M. Muthana, S. D. Scott, N. Farrow, F. Morrow, C. Murdoch, S. Grubb, N. Brown, J. Dobson, C. E. Lewis, *Gene Ther.* **2008**, *15*, 902.
[35] T. R. Pisanic Ii, J. D. Blackwell, V. I. Shubayev, R. R. Fiñones, S. Jin, *Biomaterials* **2007**, *28*, 2572.
[36] M. Chorny, I. S. Alferiev, I. Fishbein, J. E. Tengood, Z. Folchman-Wagner, S. P. Forbes, R. J. Levy, *Pharm. Res.* **2012**, *29*, 1232.
[37] M. Chorny, B. Polyak, I. S. Alferiev, K. Walsh, G. Friedman, R. J. Levy, *FASEB J.* **2007**, *21*, 2510.
[38] R. Sharma, S. Saini, P. R. Ros, P. F. Hahn, W. C. Small, E. E. de Lange, A. E. Stillman, R. R. Edelman, V. M. Runge, E. K. Outwater, M. Morris, M. Lucas, *J. Magn. Reson. Imaging* **1999**, *9*, 291.
[39] H. Lee, E. Lee, K. Do Kyung, N. K. Jang, Y. Y. Jeong, S. Jon, *J. Am. Chem. Soc.* **2006**, *128*, 7383.
[40] A. S. Arbab, L. B. Wilson, P. Ashari, E. K. Jordan, B. K. Lewis, J. A. Frank, *NMR Biomed.* **2005**, *18*, 383.
[41] L. Lartigue, D. Alloyeau, J. Kolosnjaj-Tabi, Y. Javed, P. Guardia, A. Riedinger, C. Pechoux, T. Pellegrino, C. Wilhelm, F. Gazeau, *ACS Nano* **2013**.
[42] M. Lévy, F. Lagarde, V.-A. Maraloiu, M.-G. Blanchin, F. Gendron, C. Wilhelm, F. Gazeau, *Nanotechnology* **2010**, *21*, 395103.
[43] W. P. Miller, L. W. Zelazny, D. C. Martens, *Geoderma* **1986**, *37*, 1.
[44] D. Panias, M. Taxiarchou, I. Paspaliaris, A. Kontopoulos, *Hydrometallurgy* **1996**, *42*, 257.
[45] K. Avgoustakis, A. Beletsi, Z. Panagi, P. Klepetsanis, A. G. Karydas, D. S. Ithakissios, *J. Controlled Release* **2002**, *79*, 123.
[46] F. Alexis, *Polym. Int.* **2005**, *54*, 36.
[47] B. B. Crow, A. F. Borneman, D. L. Hawkins, G. M. Smith, K. D. Nelson, *Tissue Eng.* **2005**, *11*, 1077.
[48] J. Panyam, M. M. Dali, S. K. Sahoo, W. Ma, S. S. Chakravarthi, G. L. Amidon, R. J. Levy, V. Labhasetwar, *J. Controlled Release* **2003**, *92*, 173.

[49] T. Morita, K. Takeda, K. Okumura, *Mutation Research/Genetic Toxicology* **1990**, *240*, 195.
[50] S. Boutry, D. Forge, C. Burtea, I. Mahieu, O. Murariu, S. Laurent, L. Vander Elst, R. N. Muller, *Contrast Media Mol. Imaging* **2009**, *4*, 299.
[51] J. M. Anderson, M. S. Shive, *Biodegradable Microspheres/Therapeutic Peptide Delivery* **1997**, *28*, 5.
[52] K. Fu, D. W. Pack, A. M. Klibanov, R. Langer, *Pharm. Res.* **2000**, *17*, 100.
[53] V. Mironov, V. Kasyanov, R. R. Markwald, *Trends Biotechnol.* **2008**, *26*, 338.
[54] V. Mironov, V. Kasyanov, R. R. Markwald, *Tissue Cell Pathway Eng.* **2011**, *22*, 667.
[55] V. Mironov, R. P. Visconti, V. Kasyanov, G. Forgacs, C. J. Drake, R. R. Markwald, *Biomaterials* **2009**, *30*, 2164.
[56] K. Rege, I. L. Medintz, *Methods in Bioengineering: Nanoscale Bioengineering and Nanomedicine*, Artech House, Inc. Norwood, MA **2009**.
[57] L. Ngaboni Okassa, H. Marchais, L. Douziech-Eyrolles, S. Cohen-Jonathan, M. Souce, P. Dubois, I. Chourpa, *Int. J. Pharm.* **2005**, *302*, 187.
[58] J. Cheng, B. A. Teply, I. Sherifi, J. Sung, G. Luther, F. X. Gu, E. Levy-Nissenbaum, A. F. Radovic-Moreno, R. Langer, O. C. Farokhzad, *Biomaterials* **2007**, *28*, 869.